Editors' Suggestion

Calculation of the Hadronic Vacuum Polarization Contribution to the Muon Anomalous Magnetic Moment

T. Blum,[1] P. A. Boyle,[2] V. Gülpers,[3] T. Izubuchi,[4,5] L. Jin,[1,5] C. Jung,[4] A. Jüttner,[3] C. Lehner,[4,*] A. Portelli,[2] and J. T. Tsang[2]

(RBC and UKQCD Collaborations)

[1]*Physics Department, University of Connecticut, Storrs, Connecticut 06269-3046, USA*
[2]*School of Physics and Astronomy, The University of Edinburgh, Edinburgh EH9 3FD, United Kingdom*
[3]*School of Physics and Astronomy, University of Southampton, Southampton SO17 1BJ, United Kingdom*
[4]*Physics Department, Brookhaven National Laboratory, Upton, New York 11973, USA*
[5]*RIKEN-BNL Research Center, Brookhaven National Laboratory, Upton, New York 11973, USA*

(Received 25 January 2018; published 12 July 2018)

We present a first-principles lattice QCD + QED calculation at physical pion mass of the leading-order hadronic vacuum polarization contribution to the muon anomalous magnetic moment. The total contribution of up, down, strange, and charm quarks including QED and strong isospin breaking effects is $a_\mu^{\mathrm{HVP\ LO}} = 715.4(18.7) \times 10^{-10}$. By supplementing lattice data for very short and long distances with R-ratio data, we significantly improve the precision to $a_\mu^{\mathrm{HVP\ LO}} = 692.5(2.7) \times 10^{-10}$. This is the currently most precise determination of $a_\mu^{\mathrm{HVP\ LO}}$.

DOI: 10.1103/PhysRevLett.121.022003

Introduction.—The anomalous magnetic moment of the muon a_μ is defined as the deviation of the Landé factor g_μ from Dirac's relativistic quantum mechanics result, $a_\mu = [(g_\mu - 2)/2]$. It is one of the most precisely determined quantities in particle physics and is currently known both experimentally (BNL E821) [1] and from a standard model theory calculation [2] to approximately 1/2 parts per million.

Interestingly, the standard model result a_μ^{SM} deviates from the experimental measurement a_μ^{expt} at the 3–4σ level, depending on which determination of the leading-order hadronic vacuum polarization $a_\mu^{\mathrm{HVP\ LO}}$ is used. One finds [3–6]

$$\begin{aligned} a_\mu^{\mathrm{expt}} - a_\mu^{\mathrm{SM}} &= 25.0(4.3)(2.6)(6.3) \times 10^{-10}\ [3,4], \\ &\quad 31.8(4.1)(2.6)(6.3) \times 10^{-10}\ [4,5], \\ &\quad 26.8(3.4)(2.6)(6.3) \times 10^{-10}\ [4,6], \end{aligned} \tag{1}$$

where the quoted errors correspond to the uncertainty in $a_\mu^{\mathrm{HVP\ LO}}$, $a_\mu^{\mathrm{SM}} - a_\mu^{\mathrm{HVP\ LO}}$, and a_μ^{expt}. This tension may hint at new physics beyond the standard model of particle physics such that a reduction of uncertainties in Eq. (1) is highly desirable. New experiments at Fermilab (E989) [7] and J-PARC (E34) [8] intend to decrease the experimental uncertainty by a factor of 4. First results of the E989 experiment may be available before the end of 2018 [9] such that a reduction in uncertainty of the $a_\mu^{\mathrm{HVP\ LO}}$ contribution is of timely interest.

In the following, we perform a complete first-principles calculation of $a_\mu^{\mathrm{HVP\ LO}}$ in lattice QCD + QED at physical pion mass with nondegenerate up and down quark masses and present results for the up, down, strange, and charm quark contributions. Our lattice calculation of the light-quark QED correction to $a_\mu^{\mathrm{HVP\ LO}}$ is the first such calculation performed at physical pion mass. In addition, we replace lattice data at very short and long distances by experimental e^+e^- scattering data using the compilation of Ref. [10], which allows us to produce the currently most precise determination of $a_\mu^{\mathrm{HVP\ LO}}$.

Computational method.—The general setup of our nonperturbative lattice computation is described in Ref. [11]. We compute

$$a_\mu = 4\alpha^2 \int_0^\infty dq^2 f(q^2)[\Pi(q^2) - \Pi(q^2 = 0)], \tag{2}$$

where $f(q^2)$ is a known analytic function [11] and $\Pi(q^2)$ is defined as $\sum_x e^{iqx}\langle J_\mu(x) J_\nu(0)\rangle = (\delta_{\mu\nu} q^2 - q_\mu q_\nu)\Pi(q^2)$ with sum over space-time coordinate x and $J_\mu(x) = i \sum_f Q_f \bar{\Psi}_f(x)\gamma_\mu \Psi_f(x)$. The sum is over up, down, strange, and charm quark flavors with QED charges $Q_{\mathrm{up,charm}} = 2/3$ and $Q_{\mathrm{down,strange}} = -1/3$. For convenience we do not explicitly write the superscript HVP LO. We compute $\Pi(q^2)$ using the kernel function of Refs. [12,13]

$$\Pi(q^2) - \Pi(q^2 = 0) = \sum_t \left(\frac{\cos(qt) - 1}{q^2} + \frac{1}{2} t^2 \right) C(t) \quad (3)$$

with $C(t) = \frac{1}{3} \sum_{\vec{x}} \sum_{j=0,1,2} \langle J_j(\vec{x}, t) J_j(0) \rangle$. With appropriate definition of w_t, we can therefore write

$$a_\mu = \sum_t w_t C(t). \quad (4)$$

The correlator $C(t)$ is computed in lattice QCD + QED with dynamical up, down, and strange quarks and non-degenerate up and down quark masses. We compute the missing contributions to a_μ from bottom quarks and from charm sea quarks in perturbative QCD [14] by integrating the timelike region above 2 GeV and find them to be smaller than 0.3×10^{-10}.

We tune the bare up, down, and strange quark masses m_{up}, m_{down}, and m_{strange} such that the π^0, π^+, K^0, and K^+ meson masses computed in our calculation agree with the respective experimental measurements [15]. The lattice spacing is determined by setting the Ω^- mass to its experimental value. We perform the calculation as a perturbation around an isospin-symmetric lattice QCD computation [16,17] with two degenerate light quarks with mass m_{light} and a heavy quark with mass m_{heavy} tuned to produce a pion mass of 135.0 MeV and a kaon mass of 495.7 MeV [18]. The correlator is expanded in the fine-structure constant α as well as $\Delta m_{\text{up,down}} = m_{\text{up,down}} - m_{\text{light}}$, and $\Delta m_{\text{strange}} = m_{\text{strange}} - m_{\text{heavy}}$. We write

$$C(t) = C^{(0)}(t) + \alpha C^{(1)}_{\text{QED}}(t) + \sum_f \Delta m_f C^{(1)}_{\Delta m_f}(t) + O(\alpha^2, \alpha \Delta m, \Delta m^2), \quad (5)$$

where $C^{(0)}(t)$ is obtained in the lattice QCD calculation at the isospin symmetric point and the expansion terms define the QED and strong isospin-breaking (SIB) corrections, respectively. We keep only the leading corrections in α and Δm_f which is sufficient for the desired precision.

We insert the photon-quark vertices perturbatively with photons coupled to local lattice vector currents multiplied by the renormalization factor Z_V [18]. We use $Z_A \approx Z_V$ for the charm [19] and QED corrections. The SIB correction is computed by inserting scalar operators in the respective quark lines. The procedure used for effective masses in such a perturbative expansion is explained in Ref. [20]. We use the finite-volume QED$_L$ prescription [21] and remove the universal $1/L$ and $1/L^2$ corrections to the masses [22] with spatial lattice size L. The effect of $1/L^3$ corrections is small compared to our statistical uncertainties. We find $\Delta m_{\text{up}} = -0.00050(1)$, $\Delta m_{\text{down}} = 0.00050(1)$, and $\Delta m_{\text{strange}} = -0.0002(2)$ for the 48I lattice ensemble described in Ref. [18]. The shift of the Ω^- mass due to the QED correction is significantly smaller than the lattice spacing uncertainty and its effect on $C(t)$ is therefore not included separately.

Figure 1 shows the quark-connected and quark-disconnected contributions to $C^{(0)}$. Similarly, Fig. 2 shows the relevant diagrams for the QED correction to the meson spectrum and the hadronic vacuum polarization. The external vertices are pseudoscalar operators for the former and vector operators for the latter. We refer to diagrams S and V as the QED-connected and to diagram F as the QED-disconnected contribution. We note that only the parts of diagram F with additional gluons exchanged between the two quark loops contribute to $a_\mu^{\text{HVP LO}}$ as otherwise an internal cut through a single photon line is possible, which is part of $a_\mu^{\text{HVP NLO}}$ [23]. For this reason, we subtract the separate quantum-averages of quark loops in diagram F. In the current calculation, we neglect diagrams T, D1, D2, and D3. This approximation is estimated to yield an $O(10\%)$ correction for isospin splittings [24] for which the neglected diagrams are both SU(3) and $1/N_c$ suppressed. For the hadronic vacuum polarization the contribution of neglected diagrams is still $1/N_c$ suppressed and we adopt a corresponding 30% uncertainty.

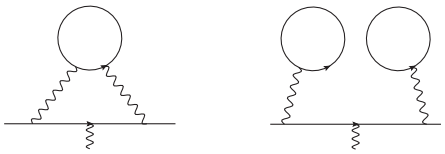

FIG. 1. Quark-connected (left) and quark-disconnected (right) diagram for the calculation of $a_\mu^{\text{HVP LO}}$. We do not draw gluons but consider each diagram to represent all orders in QCD.

In Fig. 3, we show the SIB diagrams. In the calculation presented here, we only include diagram M. For the meson masses this corresponds to neglecting the sea quark mass correction, which we have previously [18] determined to be an $O(2\%)$ and $O(14\%)$ effect for the pions and kaons, respectively. This estimate is based on the analytic fits of (H7) and (H9) of Ref. [18] with ratios $C_2^{m_{\pi,K}}/C_1^{m_{\pi,K}}$ given in Tab. XVII of the same reference. For the hadronic vacuum polarization the contribution of diagram R is negligible since $\Delta m_{\text{up}} \approx -\Delta m_{\text{down}}$ and diagram O is SU(3) and $1/N_c$ suppressed. We therefore assign a corresponding 10% uncertainty to the SIB correction.

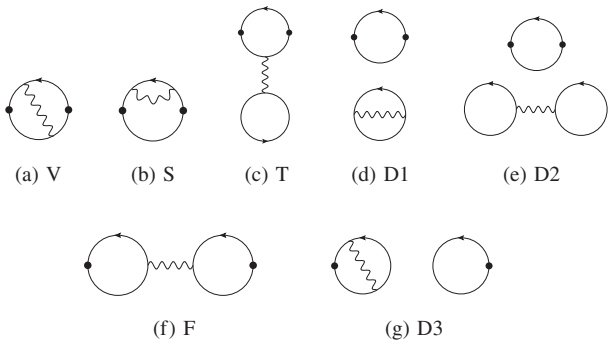

FIG. 2. QED-correction diagrams with external pseudoscalar or vector operators. The figure parts (a)–(g) assign labels V, S, T, D1, D2, F, and D3 to the respective diagrams.

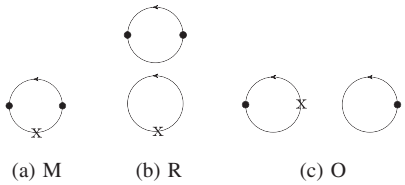

FIG. 3. Strong isospin-breaking correction diagrams. The crosses denote the insertion of a scalar operator. The figure parts (a)–(c) assign labels M, R, and O to the respective diagrams.

We also compute the $O(\alpha)$ correction to the vector current renormalization factor Z_V used in $C^{(0)}$ [18,20] and find a small correction of approximately 0.05% for the light quarks.

We perform the calculation of $C^{(0)}$ on the 48I and 64I ensembles described in Ref. [18] for the up, down, and strange quark-connected contributions. For the charm contribution we also perform a global fit using additional ensembles described in Ref. [19]. The quark-disconnected contribution as well as QED and SIB corrections are computed only on ensemble 48I.

For the noisy light quark connected contribution, we employ a multistep approximation scheme with low-mode averaging [25] over the entire volume and two levels of approximations in a truncated deflated solver with all mode averaging (AMA) [26–29] of randomly positioned point sources. The low-mode space is generated using a new Lanczos method working on multiple grids [30]. Our improved statistical estimator for the quark disconnected diagrams is described in Ref. [31] and our strategy for the strange quark is published in Ref. [32]. For diagram F, we reuse point-source propagators generated in Ref. [33].

The correlator $C(t)$ is related to the R-ratio data [12] by $C(t) = [1/(12\pi^2)] \int_0^\infty d(\sqrt{s}) R(s) s e^{-\sqrt{s}t}$ with $R(s) = [(3s)/4\pi\alpha^2]\sigma(s, e^+e^- \to \text{had})$. In Fig. 4 we compare a lattice and R-ratio evaluation of $w_t C(t)$ and note that the R-ratio data is most precise at very short and long distances, while the lattice data is most precise at intermediate distances. We are therefore led to also investigate a position-space "window method" [12,34] and write

$$a_\mu = a_\mu^{\mathrm{SD}} + a_\mu^{W} + a_\mu^{\mathrm{LD}} \tag{6}$$

with $a_\mu^{\mathrm{SD}} = \sum_t C(t) w_t [1 - \Theta(t, t_0, \Delta)]$, $a_\mu^{W} = \sum_t C(t) w_t [\Theta(t, t_0, \Delta) - \Theta(t, t_1, \Delta)]$, and $a_\mu^{\mathrm{LD}} = \sum_t C(t) \times w_t \Theta(t, t_1, \Delta)$, where each contribution is accessible from

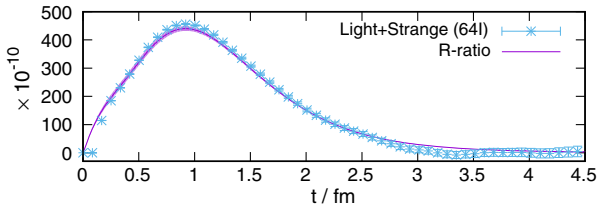

FIG. 4. Comparison of $w_t C(t)$ obtained using R-ratio data [10] and lattice data on our 64I ensemble.

both lattice and R-ratio data. We define $\Theta(t, t', \Delta) = \{1 + \tanh[(t - t')/\Delta]\}/2$ which we find to be helpful to control the effect of discretization errors by the smearing parameter Δ. We then take a_μ^{SD} and a_μ^{LD} from the R-ratio data and a_μ^{W} from the lattice. In this work we use $\Delta = 0.15$ fm, which we find to provide a sufficiently sharp transition without increasing discretization errors noticeably. This method takes the most precise regions of both data sets and therefore may be a promising alternative to the proposal of Ref. [35].

Analysis and results.—Table I shows our results for the window method and pure lattice determination. We quote statistical uncertainties for the lattice data labeled as (S) and the R-ratio data labeled as (RST) separately. Lattice and R-ratio uncertainties are added in quadrature. For the quark-connected up, down, and strange contributions, the computation is performed on two ensembles with inverse lattice spacing $a^{-1} = 1.730(4)$ GeV (48I) as well as $a^{-1} = 2.359(7)$ GeV (64I) and a continuum limit is taken. The discretization error (C) is estimated by taking the maximum of the squared measured $O(a^2)$ correction as well as a simple $(a\Lambda)^4$ estimate, where we take $\Lambda = 400$ MeV. We find the results on the 48I ensemble to differ only a few percent from the continuum limit. This holds for the full lattice contribution as well as the window contributions considered in this work. For the quark-connected charm contribution, additional ensembles described in Ref. [19] are used and the maximum of the above, and a $(am_c)^4$ estimate is taken as discretization error. The remaining contributions are small and only computed on the 48I ensemble for which we take $(a\Lambda)^2$ as estimate of discretization errors.

For the up and down quark-connected and disconnected contributions, we correct finite-volume effects to leading order in finite-volume position-space chiral perturbation theory [36]. Note that in our previous publication of the quark-disconnected contribution [31], we added this finite-volume correction as an uncertainty but did not shift the central value. We take the largest ratio of p^6 to p^4 corrections of Tab. 1 of Ref. [37] as systematic error estimate of neglected finite-volume errors (V). For the SIB correction we also include the sizable difference of the corresponding finite and infinite-volume chiral perturbation theory calculation as finite-volume uncertainty. For the QED correction, we repeat the computation using an infinite-volume photon (QED_∞ [38]) and include the difference to the QED_L result as a finite-volume error. Further details of the QED_∞ procedure are provided as Supplemental Material [39].

We furthermore propagate uncertainties of the lattice spacing (A) and the renormalization factors Z_V (Z). For the quark-disconnected contribution we adopt the additional long-distance error discussed in Ref. [31] (L) and for the charm contribution we propagate uncertainties from the global fit procedure [19] (M). Systematic errors of the R-ratio computation are taken from Ref. [10] and quoted as

TABLE I. Individual and summed contributions to a_μ multiplied by 10^{10}. The left column lists results for the window method with $t_0 = 0.4$ fm and $t_1 = 1$ fm. The right column shows results for the pure first-principles lattice calculation. The respective uncertainties are defined in the main text.

$a_\mu^{\text{ud,conn,isospin}}$	$202.9(1.4)_S(0.2)_C(0.1)_V(0.2)_A(0.2)_Z$	$649.7(14.2)_S(2.8)_C(3.7)_V(1.5)_A(0.4)_Z(0.1)_{\text{E48}}(0.1)_{\text{E64}}$
$a_\mu^{\text{s,conn,isospin}}$	$27.0(0.2)_S(0.0)_C(0.1)_A(0.0)_Z$	$53.2(0.4)_S(0.0)_C(0.3)_A(0.0)_Z$
$a_\mu^{\text{c,conn,isospin}}$	$3.0(0.0)_S(0.1)_C(0.0)_Z(0.0)_M$	$14.3(0.0)_S(0.7)_C(0.1)_Z(0.0)_M$
$a_\mu^{\text{uds,disc,isospin}}$	$-1.0(0.1)_S(0.0)_C(0.0)_V(0.0)_A(0.0)_Z$	$-11.2(3.3)_S(0.4)_V(2.3)_L$
$a_\mu^{\text{QED,conn}}$	$0.2(0.2)_S(0.0)_C(0.0)_V(0.0)_A(0.0)_Z(0.0)_E$	$5.9(5.7)_S(0.3)_C(1.2)_V(0.0)_A(0.0)_Z(1.1)_E$
$a_\mu^{\text{QED,disc}}$	$-0.2(0.1)_S(0.0)_C(0.0)_V(0.0)_A(0.0)_Z(0.0)_E$	$-6.9(2.1)_S(0.4)_C(1.4)_V(0.0)_A(0.0)_Z(1.3)_E$
a_μ^{SIB}	$0.1(0.2)_S(0.0)_C(0.2)_V(0.0)_A(0.0)_Z(0.0)_{\text{E48}}$	$10.6(4.3)_S(0.6)_C(6.6)_V(0.1)_A(0.0)_Z(1.3)_{\text{E48}}$
$a_\mu^{\text{udsc,isospin}}$	$231.9(1.4)_S(0.2)_C(0.1)_V(0.3)_A(0.2)_Z(0.0)_M$	$705.9(14.6)_S(2.9)_C(3.7)_V(1.8)_A(0.4)_Z(2.3)_L(0.1)_{\text{E48}}(0.1)_{\text{E64}}(0.0)_M$
$a_\mu^{\text{QED,SIB}}$	$0.1(0.3)_S(0.0)_C(0.2)_V(0.0)_A(0.0)_Z(0.0)_E(0.0)_{\text{E48}}$	$9.5(7.4)_S(0.7)_C(6.9)_V(0.1)_A(0.0)_Z(1.7)_E(1.3)_{\text{E48}}$
$a_\mu^{R-\text{ratio}}$	$460.4(0.7)_{\text{RST}}(2.1)_{\text{RSY}}$	
a_μ	$692.5(1.4)_S(0.2)_C(0.2)_V(0.3)_A(0.2)_Z(0.0)_E(0.0)_{\text{E48}}$	$715.4(16.3)_S(3.0)_C(7.8)_V(1.9)_A(0.4)_Z(1.7)_E(2.3)_L$
	$(0.0)_b(0.1)_c(0.0)_{\bar{S}}(0.0)_{\bar{Q}}(0.0)_M(0.7)_{\text{RST}}(2.1)_{\text{RSY}}$	$(1.5)_{\text{E48}}(0.1)_{\text{E64}}(0.3)_b(0.2)_c(1.1)_{\bar{S}}(0.3)_{\bar{Q}}(0.0)_M$

(RSY). The neglected bottom quark (b) and charm sea quark (c) contributions as well as effects of neglected QED ($\bar{Q}$) and SIB ($\bar{S}$) diagrams are estimated as described in the previous section.

For the QED and SIB corrections, we assume dominance of the low-lying $\pi\pi$ and $\pi\gamma$ states and fit $C^{(1)}_{\text{QED}}(t)$ as well as $C^{(1)}_{\Delta m_f}(t)$ to $(c_1 + c_0 t)e^{-Et}$, where we vary c_0 and c_1 for fixed energy E. The resulting p values are larger than 0.2 for all cases and we use this functional form to compute the respective contribution to a_μ. For the QED correction, we vary the energy E between the lowest $\pi\pi$ and $\pi\gamma$ energies and quote the difference as additional uncertainty (E). For the SIB correction, we take E to be the $\pi\pi$ ground-state energy.

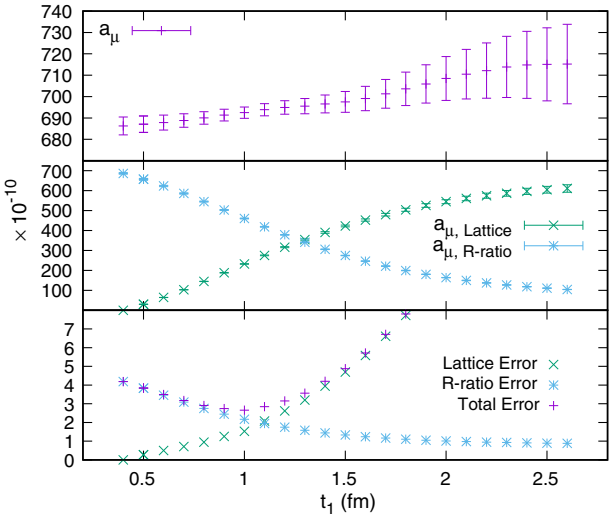

FIG. 5. We show results for the window method with $t_0 = 0.4$ fm as a function of t_1. The top panel shows the combined a_μ, the middle panel shows the partial contributions of the lattice and R-ratio data, and the bottom shows the respective uncertainties.

For the light quark contribution of our pure lattice result we use a bounding method [42] similar to Ref. [43] and find that upper and lower bounds meet within errors at $t = 3.0$ fm. We vary the ground-state energy that enters this method [44] between the free-field and interacting value [45]. For the 48I ensemble we find $E_0^{\text{free}} = 527.3$ MeV, $E_0 = 517.4$ MeV $+ O(1/L^6)$ and for the 64I ensemble we have $E_0^{\text{free}} = 536.1$ MeV, $E_0 = 525.1$ MeV $+ O(1/L^6)$. We quote the respective uncertainties as (E48) and (E64). The variation of $\pi\pi$ ground-state energy on the 48I ensemble also enters the SIB correction as described above.

Figure 5 shows our results for the window method with $t_0 = 0.4$ fm. While the partial lattice and R-ratio contributions change by several 100×10^{-10}, the sum changes only at the level of quoted uncertainties. This provides a nontrivial consistency check between the lattice and the R-ratio data for length scales between 0.4 fm and 2.6 fm. We expand on this check in the Supplemental Material [39]. The uncertainty of the current analysis is minimal for $t_1 = 1$ fm, which we take as our main result for the window method. For $t_0 = t_1$ we reproduce the value of Ref. [10]. In Fig. 6, we show the t_1 dependence of individual lattice contributions and compare our results with previously published results in Fig. 7. Our combined

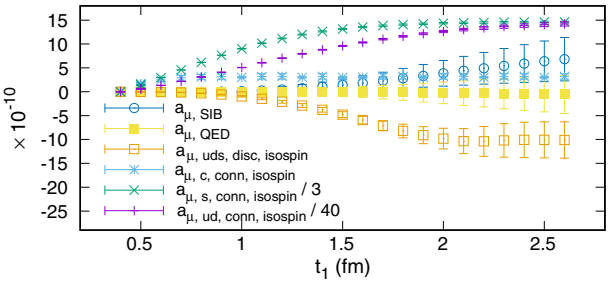

FIG. 6. The individual lattice components of the window method with $t_0 = 0.4$ fm as function of t_1.

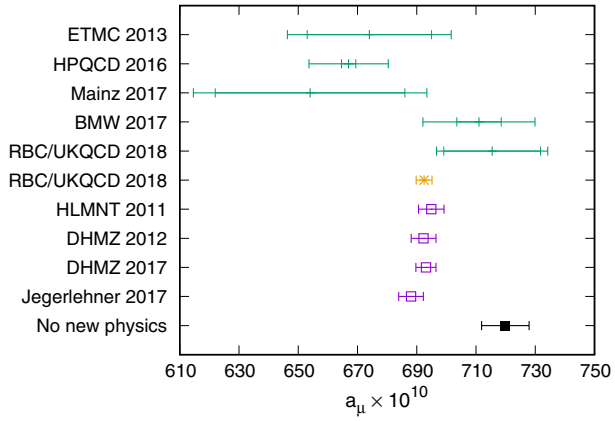

FIG. 7. Our results (RBC and UKQCD 2018) compared to previously published results. The green data points are pure lattice computations, the orange data point is our combined window analysis, and the purple data points are pure R-ratio results. The references are ETMC 2013 [46], HPQCD 2016 [47], Mainz 2017 [48], BMW 2017 [44], HLMNT 2011 [3], DHMZ 2012 [49], DHMZ 2017 [6], Jegerlehner 2017 [5], and No new physics [2]. The innermost error bar corresponds to the statistical uncertainty.

lattice and R-ratio result is more precise than the R-ratio computation by itself and reduces the tension to the other R-ratio results. Results for different window parameters t_0 and t_1 and a comparison of individual components with previously published results are provided as Supplemental Material [39].

Conclusion.—We have presented both a complete first-principles calculation of the leading-order hadronic vacuum polarization contribution to the muon anomalous magnetic moment from lattice QCD + QED at physical pion mass as well as a combination with R-ratio data. For the former we find $a_\mu^{\mathrm{HVP\ LO}} = 715.4(16.3)(9.2) \times 10^{-10}$, where the first error is statistical and the second is systematic. For the latter we find $a_\mu^{\mathrm{HVP\ LO}} = 692.5(1.4)(0.5)(0.7)(2.1) \times 10^{-10}$ with lattice statistical, lattice systematic, R-ratio statistical, and R-ratio systematic errors given separately. This is the currently most precise determination of $a_\mu^{\mathrm{HVP\ LO}}$ corresponding to a 3.7σ tension

$$a_\mu^{\mathrm{expt}} - a_\mu^{\mathrm{SM}} = 27.4(2.7)(2.6)(6.3) \times 10^{-10}\ [4]. \quad (7)$$

The presented combination of lattice and R-ratio data also serves to provide additional nontrivial cross-checks between lattice and R-ratio data. The precision of this computation will be improved in future work by adding the missing subleading QED and SIB diagrams and simulations at smaller lattice spacings and larger volumes.

We would like to thank our RBC and UKQCD collaborators for helpful discussions and support. We would also like to thank Kim Maltman and Masashi Hayakawa for valuable discussions. We are indebted to Fred Jegerlehner for helpful exchanges on the R-ratio compilation of Ref. [10]. P. A. B., A. P., and J. T. T. are supported in part by UK STFC Grants No. ST/L000458/1 and No. ST/P000630/1. A. P. also received funding from the European Research Council (ERC) under the European Union's Horizon 2020 research and innovation programme under Grant Agreement No. 757646. T. B. is supported by U.S. Department of Energy Grant No. DE-FG02-92ER40716. V. G. and A. J. acknowledge support from STFC consolidated Grant No. ST/P000711/1, A. J. has also received funding from the European Research Council under the EU FP7 Programme (FP7/2007-2013) / ERC Grant Agreement No. 279757. T. I., C. J., and C. L. are supported in part by US DOE Contract No. DESC0012704(BNL). T. I. is also supported by JSPS KAKENHI Grants No. JP26400261, No. JP17H02906, and by MEXT as "Priority Issue on Post-K computer" (Elucidation of the Fundamental Laws and Evolution of the Universe) and Joint Institute for Computational Fundamental Science. C. L. is also supported by a DOE Office of Science Early Career Award. L. J. is supported by the Department of Energy, Laboratory Directed Research and Development (LDRD) funding of BNL, under Contract No. DE-EC0012704. This work was supported by resources provided by the Scientific Data and Computing Center (SDCC) at Brookhaven National Laboratory (BNL), a DOE Office of Science User Facility supported by the Office of Science of the US Department of Energy. The SDCC is a major component of the Computational Science Initiative at BNL. We gratefully acknowledge computing resources provided through USQCD clusters at Fermilab and Jefferson Lab as well as the IBM Blue Gene/Q (BG/Q) Mira machine at the Argonne Leadership Class Facility, a DOE Office of Science Facility supported under Contract No. De-AC02-06CH11357. This work was also supported by the Distributed Research utilizing Advanced Computing Blue Gene Q Shared Petaflop system at the University of Edinburgh, operated by the Edinburgh Parallel Computing Centre on behalf of the STFC DiRAC HPC Facility [50]. This equipment was funded by BIS National E-infrastructure capital Grant No. ST/K000411/1, STFC capital Grant No. ST/H008845/1, and STFC DiRAC Operations Grants No. ST/K005804/1 and No. ST/K005790/1. DiRAC is part of the National E-Infrastructure. The software used includes BAGEL (GNU GPLv2 license), CPS, GPT, GRID (GNU GPLv2 license), and LATANALYZE (GNU GPLv3 license).

*Corresponding author.
clehner@quark.phy.bnl.gov

[1] G. Bennett *et al.* (Muon G-2 Collaboration), Phys. Rev. D **73**, 072003 (2006).
[2] C. Patrignani *et al.* (Particle Data Group), Chin. Phys. C **40**, 100001 (2016), including the 2017 update for the 2016 edition at http://pdg.lbl.gov.

[3] K. Hagiwara, R. Liao, A. D. Martin, D. Nomura, and T. Teubner, J. Phys. G **38**, 085003 (2011).
[4] J. Prades, E. de Rafael, and A. Vainshtein, Adv. Ser. Dir. High Energy Phys. **20**, 303 (2009).
[5] F. Jegerlehner, Eur. Phys. J. Web Conf. **166**, 00022 (2018).
[6] M. Davier, A. Hoecker, B. Malaescu, and Z. Zhang, Eur. Phys. J. C **77**, 827 (2017).
[7] R. Carey *et al.*, The New (g-2) Experiment: A proposal to measure the muon anomalous magnetic moment to +-0.14 ppm precision, 2009, DOI: 10.2172/952029.
[8] M. Aoki *et al.*, KEK-J-PARC **PAC2009**, 12 (2009).
[9] Fermilab E989 Collaboration (private communication).
[10] F. Jegerlehner, alphaQEDc17, 2017, http://www-com.physik.hu-berlin.de/~fjeger/software.html.
[11] T. Blum, Phys. Rev. Lett. **91**, 052001 (2003).
[12] D. Bernecker and H. B. Meyer, Eur. Phys. J. A **47**, 148 (2011).
[13] X. Feng, S. Hashimoto, G. Hotzel, K. Jansen, M. Petschlies, and D. B. Renner, Phys. Rev. D **88**, 034505 (2013).
[14] R. V. Harlander and M. Steinhauser, Comput. Phys. Commun. **153**, 244 (2003).
[15] We minimize the sum of squared differences of computed and measured meson masses.
[16] G. M. de Divitiis *et al.*, J. High Energy Phys. 04 (2012) 124.
[17] G. M. de Divitiis, R. Frezzotti, V. Lubicz, G. Martinelli, R. Petronzio, G. C. Rossi, F. Sanfilippo, S. Simula, and N. Tantalo (RM123 Collaboration), Phys. Rev. D **87**, 114505 (2013).
[18] T. Blum *et al.* (RBC and UKQCD Collaborations), Phys. Rev. D **93**, 074505 (2016).
[19] P. A. Boyle, L. Del Debbio, A. Jüttner, A. Khamseh, F. Sanfilippo, and J. T. Tsang, J. High Energy Phys. 12 (2017) 008.
[20] P. Boyle, V. Gülpers, J. Harrison, A. Jüttner, C. Lehner, A. Portelli, and C. T. Sachrajda, J. High Energy Phys. 09 (2017) 153.
[21] M. Hayakawa and S. Uno, Prog. Theor. Phys. **120**, 413 (2008).
[22] S. Borsanyi *et al.*, Science **347**, 1452 (2015).
[23] K. Hagiwara, A. D. Martin, D. Nomura, and T. Teubner, Phys. Rev. D **69**, 093003 (2004).
[24] S. Borsanyi *et al.*, Phys. Rev. Lett. **111**, 252001 (2013).
[25] T. A. DeGrand and S. Schäfer, Nucl. Phys. B, Proc. Suppl. **140**, 296 (2005).
[26] S. Collins, G. Bali, and A. Schäfer, Proc. Sci., LATTICE2007 (**2007**) 141.
[27] G. S. Bali, S. Collins, and A. Schäfer, Comput. Phys. Commun. **181**, 1570 (2010).
[28] T. Blum, T. Izubuchi, and E. Shintani, Phys. Rev. D **88**, 094503 (2013).
[29] E. Shintani, R. Arthur, T. Blum, T. Izubuchi, C. Jung, and C. Lehner, Phys. Rev. D **91**, 114511 (2015).
[30] M. A. Clark, C. Jung, and C. Lehner, Eur. Phys. J. Web Conf. **175**, 14023 (2018).
[31] T. Blum, P. A. Boyle, T. Izubuchi, L. Jin, A. Jüttner, C. Lehner, K. Maltman, M. Marinkovic, A. Portelli, and M. Spraggs, Phys. Rev. Lett. **116**, 232002 (2016).
[32] T. Blum *et al.* (RBC and UKQCD Collaborations), J. High Energy Phys. 04 (2016) 063; 05 (2017) 034.
[33] T. Blum, N. Christ, M. Hayakawa, T. Izubuchi, L. Jin, C. Jung, and C. Lehner, Phys. Rev. Lett. **118**, 022005 (2017).
[34] C. Lehner (RBC and UKQCD Collaborations), Eur. Phys. J. Web Conf. **175**, 01024 (2018).
[35] J. Charles, D. Greynat, and E. de Rafael, Phys. Rev. D **97**, 076014 (2018).
[36] C. Aubin, T. Blum, P. Chau, M. Golterman, S. Peris, and C. Tu, Phys. Rev. D **93**, 054508 (2016).
[37] J. Bijnens and J. Relefors, J. High Energy Phys. 12 (2017) 114.
[38] C. Lehner and T. Izubuchi, Proc. Sci., LATTICE2014 (**2015**) 164.
[39] See Supplemental Material at http://link.aps.org/supplemental/10.1103/PhysRevLett.121.022003 for additional details and results, which includes Refs. [40,41].
[40] D. Giusti, V. Lubicz, G. Martinelli, F. Sanfilippo, and S. Simula, J. High Energy Phys. 10 (2017) 157.
[41] B. Chakraborty *et al.* (Fermilab Lattice, HPQCD, and MILC Collaborations), Phys. Rev. Lett. **120**, 152001 (2018).
[42] C. Lehner, The hadronic vacuum polarization contribution to the muon anomalous magnetic moment, RBRC Workshop on Lattice Gauge Theories, 2016, https://indico.bnl.gov/event/1628/contributions/2819/attachments/2334/2754/Lehner-2016-03-09.pdf.
[43] S. Borsanyi, Z. Fodor, T. Kawanai, S. Krieg, L. Lellouch, R. Malak, K. Miura, K. K. Szabo, C. Torrero, and B. C. Toth, Phys. Rev. D **96**, 074507 (2017).
[44] S. Borsanyi *et al.*, preceding Letter, Phys. Rev. Lett. **121**, 022002 (2018).
[45] M. Lüscher, Commun. Math. Phys. **105**, 153 (1986).
[46] F. Burger, X. Feng, G. Hotzel, K. Jansen, M. Petschlies, and D. B. Renner (ETM Collaboration), J. High Energy Phys. 02 (2014) 099.
[47] B. Chakraborty, C. T. H. Davies, P. G. de Oliveira, J. Koponen, G. P. Lepage, and R. S. Van de Water, Phys. Rev. D **96**, 034516 (2017).
[48] M. D. Morte, A. Francis, V. Gülpers, G. Herdoíza, G. von Hippel, H. Horch, B. Jäger, H. B. Meyer, A. Nyffeler, and H. Wittig, J. High Energy Phys. 10 (2017) 020.
[49] M. Davier, A. Hoecker, B. Malaescu, and Z. Zhang, Eur. Phys. J. C **71**, 1515 (2011); **72**, 1874 (2012).
[50] www.dirac.ac.uk.